Development of three-dimensional-micro-pulling-down method and growth of spring-shaped sapphire single crystals

Journal:	*CrystEngComm*
Manuscript ID	CE-ART-06-2024-000560.R1
Article Type:	Paper
Date Submitted by the Author:	19-Jul-2024

Complete List of Authors:	Yokota, Yuui; Tohoku University, Institute for Materials Research; Ohashi, Yuji; Tohoku University New Industry Creation Hatchery Center Yoshikawa, Akira; Tohoku University Institute for Materials Research

ARTICLE

Development of three-dimensional-micro-pulling-down method and growth of spring-shaped sapphire single crystals

Received 00th January 20xx,
Accepted 00th January 20xx

DOI: 10.1039/x0xx00000x

Yuui Yokota,*[a] Yuji Ohashi [b] and Akira Yoshikawa [c]

Three-dimensional-micro-pulling-down (3D-μ-PD) method was developed for the growth of 3D shaped single crystals, and spring-shaped sapphire single crystals were grown by the 3D-μ-PD method using Mo crucibles with different dies. The shape of the die significantly affected the growth stability and shape control of the spring-shaped single crystals. Spring-shaped sapphire single crystals with a smaller helical pitch and larger helical radius were obtained easily using a Mo crucible with a sharp conical die compared to that with a blunt conical die. However, spring-shaped sapphire single crystals grown using a Mo crucible with an inverse conical die can be obtained with smaller helical pitches, and the shape of the cross-sectional plane is a horizontally extended elliptical shape. The difference in the shape of the cross-sectional plane for spring-shaped sapphire single crystals affects the crystallinity and mechanical properties. Furthermore, crystals grown using the Mo crucible with the inverse conical die exhibited larger shrinkage rate in the compression test.

1. Introduction

Various functional bulk single crystals are used in various configurations for applications in optical, electrical, medical, energy, and security devices. However, conventional melt-growth methods, such as the Czochralski (Cz),[1,2] Bridgman-Stockbarger (BS),[3,4] and Floating Zone (FZ) methods[5,6] cannot control the shape of a grown single crystal, and the forming processes for each configuration from the grown single crystal increase the manufacturing cost of single-crystal elements. Furthermore, most single crystals are easily cracked during processing (cutting and polishing), which makes it difficult to process single crystals into complex shapes. However, the edge-defined film-fed growth (EFG) method can control the configuration of the grown single crystal using a die,[7] and there are numerous reports on shape-controlled crystal growth using the EFG method.[8-11]

A micro-pulling down (μ-PD) method is one of the melt-growth methods, which can control the configuration of grown single crystals using a crucible with a die at the bottom.[12,13] During the crystal growth by the μ-PD method, the shape of meniscus can be controlled by the bottom shape of the die. Consequently, a single fiber crystal with the same cross-sectional shape as that at the bottom of the die can be obtained. There are some reports of the shape-controlled single crystals by the μ-PD method, such as fiber, plate and tube-shaped sapphire single crystals,[14] square column-shaped Ce:$Y_3Al_5O_{12}$ scintillator single crystals,[15] columnar, plate and tube-shaped piezoelectric single crystals,[16-19] and metal and alloy fibers.[20,21]

However, the conventional μ-PD method can control only the cross-sectional shape of the grown fiber single crystal;[22-25] thus, the shape-controlled growth of single crystal by the μ-PD method is a two-dimensional (2D) shape control. Therefore, we developed a modified μ-PD method, which can control the shape of the grown single crystal in three dimensions (3D) to grow a single crystal with a more complex shape. The modified growth process was named as a three-dimensional-μ-PD (3D-μ-PD) method. In this study, as a first step in 3D shape-controlled single crystals, spring-shaped sapphire single crystals were grown using the 3D-μ-PD method and the optimization of shape controllability was investigated.

2. Development of 3D-μ-PD method

Schematic diagram of the 3D-μ-PD method and developed 3D-μ-PD furnace are shown in Fig. 1(a) with the conventional μ-PD method. Whereas a growth shaft moves only in the *Z*-axis of the conventional μ-PD method. The 3D-μ-PD method has a growth shaft, which can move in three dimensions (*X*, *Y*, and *Z*-axes) and rotate (θ-axis) below the growth area. The movement of the shaft can be automatically controlled according to the predesigned shape using specialized software [Fig. 1(b)]. In this study, a control software program was designed to grow spring-shaped single crystals. However, the growth shaft can be automatically and freely controlled from the beginning to the end of crystal growth by creating a program adapted to the desired 3D structure. The metal and carbon crucibles were directly heated by a high-frequency (HF) induction coil, and the temperature of the crucible was controlled by the output of the HF generator. The crucible was surrounded by tube insulators

[a.] Institute for Materials Research, Tohoku University, 2-1-1, Katahira, Aoba-ku, Sendai, Miyagi, 980-8577, Japan. E-mail: yui.yokota.a5@tohoku.ac.jp
[b.] New Industry Creation Hatchery Center (NICHe), Tohoku University, 6-6-10, Aoba, Aramaki, Aoba-ku, Sendai, Miyagi, 980-8579, Japan.
† Footnotes relating to the title and/or authors should appear here.
Supplementary Information available: [details of any supplementary information available should be included here]. See DOI: 10.1039/x0xx00000x

made of α-Al_2O_3 or ZrO_2, and the configuration of the insulators controlled the temperature gradient along the growth direction and the temperature homogeneity in the radial direction. During crystal growth, the solid-liquid interface was observed by a charge-coupled device (CCD) camera through the holes of the after-heater and insulators in real time. The growth atmosphere was controlled by sealing it with a quartz tube and bellows after vacuuming using a dry pump.

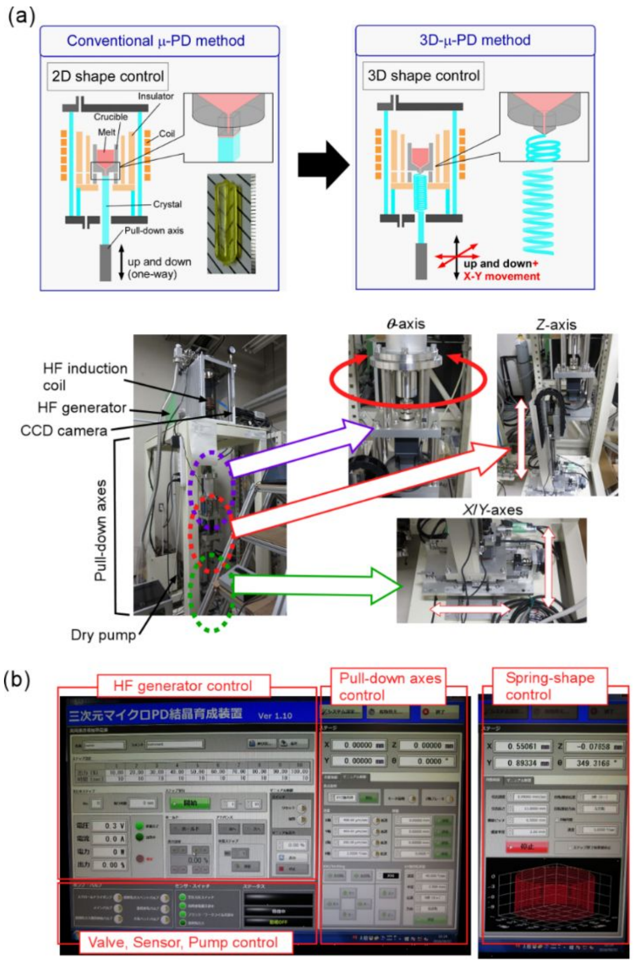

Fig. 1 (a) Schematic diagram of 3D-μ-PD method and developed 3D-μ-PD furnace. (b) Specialized control software.

3. Experiment

First, spring-shaped sapphire single crystals were grown by the 3D-μ-PD method using a Mo crucible with a conical die at the bottom. Two types of Mo crucibles with different conical dies (sharp and blunt tips) were designed as shown in Fig. 2(a). The angles between the side of the conical die and the horizontal plane in the crucibles with the sharp and blunt dies were 75.9° and 50.2°, respectively. Subsequently, a Mo crucible with an inverted conical die was designed based on the results of crystal growth using crucibles with a conical die [Fig. 2(b)]. The inverse conical die was designed to suppress the spread of the meniscus to the top during crystal growth, and the angle between the side of the inverse conical die and the horizontal plane was 135°. All crucibles had a hole (capillary) with ϕ a 0.5 mm hole at the center of each die, and the melt in the crucible reached the bottom of the die through the capillary.

A starting material, α-Al_2O_3 (>4N purity) powder, was set into the crucible as a starting material, and the crucible was heated to a melting point of α-Al_2O_3 by a high-frequency (HF) induction coil. Subsequently, the α-Al_2O_3 powder was completely melted in the crucible and the melt descended to the bottom of the die through the capillary. A sapphire single crystal with c-axis orientation was used as a seed crystal, and a crystal growth was performed at 0.5 mm/min growth rate under Ar+2%H_2 mixed gas. Ar+2%H_2 gas mixture prevented the oxidization of the Mo crucible. After the seed crystal touched the bottom of the melt, it was moved according to the setup conditions, such as helical radius and pitch, growth rate, and growth length. As described above, the movement of growth shaft was automatically controlled using the specialized software according to the predesigned shape and predetermined crystal growth rate (0.5 mm/min). During crystal growth, a solid-liquid interface was observed using a charge-coupled device (CCD) camera, and the size of the meniscus was optimally controlled by the output of the HF generator. Single crystals of the grown spring-shaped sapphire were cut perpendicular to the growth direction, and the cut surface was polished for observation and crystallinity measurements.

The polished surfaces of the spring-shaped sapphire single crystals were observed using a scanning electron microscope (SEM) (HITACHI, S-3400N), and their chemical compositions were analyzed using energy dispersive X-ray spectrometry (EDX) (HORIBA, EMAX X-act). The pole figure and X-ray rocking curve (XRC) of the polished surface were measured using an X-ray diffractometer (Bruker, D8 DISCOVERY, and Rigaku ATX-E) to evaluate the crystallinity. The pole figure and XRC were measured for reflection from the (110) plane, and ω a scan was performed during the XRC measurement. Compression tests were performed using a universal testing machine (SHIMAZU, AG-10kN) to evaluate the springiness of the spring-shaped sapphire single crystals. The specimens were compressed using a load cell in the *Z*-axis direction, and the shrinkage state until rupture was observed using a CCD camera.

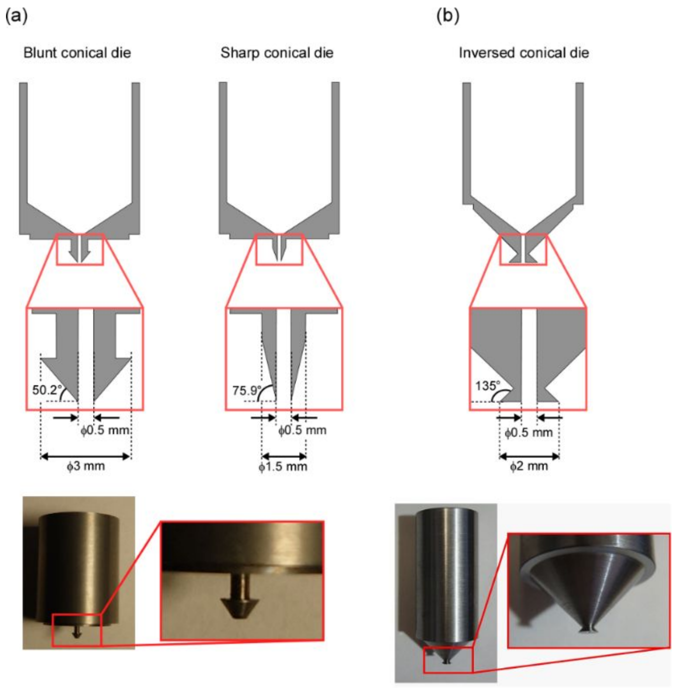

Fig. 2 Schematic diagram of Mo crucibles with (a) two-types conical dies and (b) an inversed conical die.

4. Results and discussions

4.1 Crystal growth using crucible with a conical die

The solid–liquid interface during the crystal growth of spring-shaped single crystals by the 3D-μ-PD method using Mo crucibles with blunt and sharp conical dies is shown in Fig.3(a). Figure 3(b) shows the spring-shaped sapphire single crystals grown using crucibles with conical dies. First, crystal growths were performed at growth conditions of helical radius = 1.5 mm and helical pitch = 8.0, 10.0, and 15.0 mm using the Mo crucible with the blunt conical die [Fig.3(a)]. At the growth conditions of helical pitch = 10.0, 15.0 mm, spring-shaped sapphire single crystals could be grown as shown in Fig.3(b). However, the cross-sectional shape of the spring-shaped sapphire single crystal could not be controlled under the growth conditions of a helical pitch of 8.0 mm. After the seed crystal touched the meniscus at the bottom of the die, the meniscus increased on the side of the die with the movement of the growth shaft along the helical shape. The meniscus solidified and adhered to the upper part of the die when a sufficient amount of meniscus was present. When crystal growth was performed with a smaller amount of meniscus to prevent the rise on the side of the die, the diameter of the grown single crystal gradually decreased, and crystal growth was completed.

Crystal growth of spring-shaped sapphire single crystals was performed using a Mo crucible with a sharp conical die under five growth conditions: helical radius = 1.5, 2.5, 3.0, and 3.5 mm and helical pitch (5.0, 10.0 mm) [Fig.3(a)]. In the case of the growth condition of helical radius = 1.5 mm and helical pitch = 10.0 mm, the meniscus remained on the bottom of the sharp conical die during the crystal growth. However, the meniscus spread on the side of the sharp conical die from the bottom under the growth conditions of helical radius ≥ 2.5 mm because of the tilt of the growth direction. In addition, the spread of the meniscus was limited at the edge of the sharp conical die under the growth conditions of helical radius = 2.5, 3.5 mm and helical pitch = 10.0 mm, and helical radius = 3.0 mm and helical pitch = 5.0 mm. Consequently, spring-shaped sapphire single crystals with a smaller helical pitch and larger helical radius were obtained using a crucible with a sharp die compared with a crucible with a blunt die [Fig.3(b)].

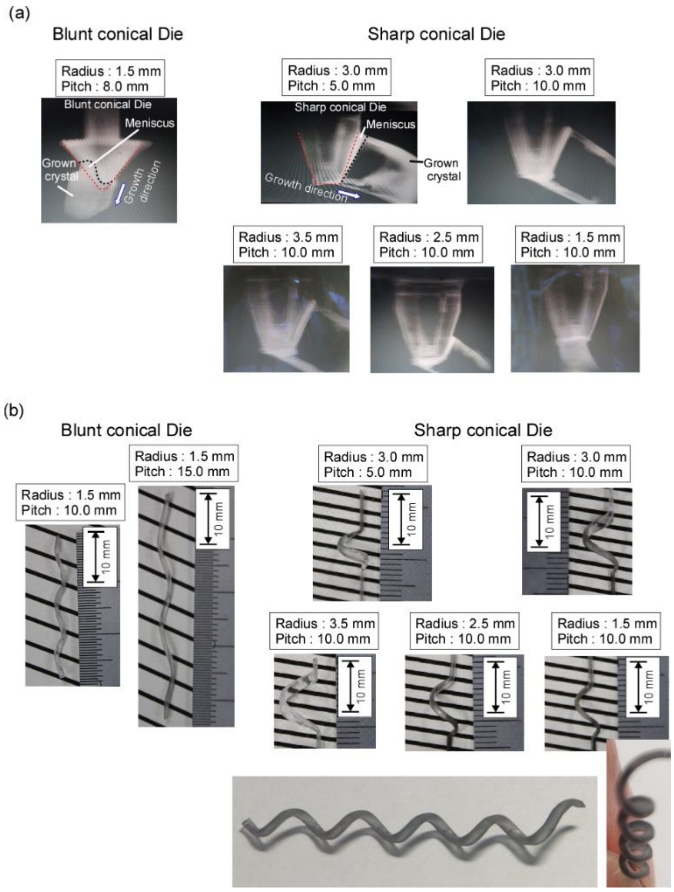

Fig. 3 (a) Solid-liquid interface during crystal growth and (b) spring-shaped sapphire single crystals grown using Mo crucibles with blunt and sharp conical dies.

4.2 Crystal growth using crucible with an inversed conical die

Based on the results of crystal growth using Mo crucibles with conical dies, a modified Mo crucible with an inverted conical die was designed, as shown in Fig. 2(b), and spring sapphire single crystals were grown using a crucible with an inverted conical die. Figure 4(a) shows the solid-liquid interface from seed-touching to stable growth during crystal growth using a Mo crucible with an inverse conical die. First, the meniscus spread to the bottom of the die; however, there was no spread of the meniscus on the side of the die during crystal growth even though the pulling shaft moved to the spring shape. Consequently, the growth of spring sapphire single crystals proceeded stably under various growth conditions.

Therefore, spring-shaped sapphire single crystals were grown in a Mo crucible with an inverted conical die under various helical pitches [Fig. 4(b)]. In the case of helical radius = 2 mm, spring-shaped sapphire single crystals could be grown at helical pitch ≥ 2 mm. However, crystal growth could not be achieved at a helical pitch of < 2 mm because of the insufficient supply of melt at the bottom of the die. Figure 4(c) shows the spring-shaped sapphire single crystals grown in a Mo crucible with an inverse conical die under various helical pitches. Spring sapphire single crystals with various helical pitches ≥ 2 mm could be obtained, and all grown crystals indicated high transparency. Under these growth conditions, the meniscus shape was stable throughout crystal growth, and the grown crystals exhibited accurate spring shapes. The stability of crystal shape was evaluated at various measurement points for the spring-shaped crystal with 3 turns, and the results showed that the error range of the shape was less than about 10% in the region of stable crystal growth.

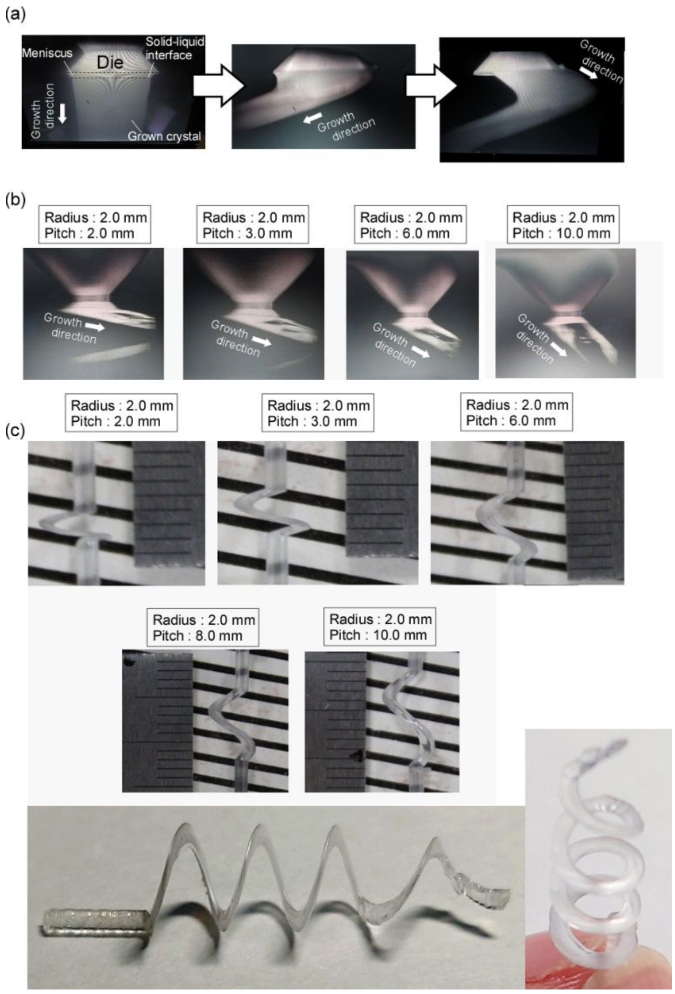

Fig. 4 (a) Solid-liquid interface from the seed-touching to the stable growth during the crystal growth using the Mo crucible with the inversed conical die. (b) Solid-liquid interface and (c) spring-shaped sapphire single crystals grown by Mo crucible with the inversed conical die under various helical pitches.

4.3 Microstructure and chemical composition analysis

Figure 5(a) shows the SEM images of the cross-sectional planes of the spring-shaped sapphire single crystals grown using a Mo crucible with a sharp conical die. The polished specimens were colorless and transparent without visible inclusions or cracks in the crystals, although there were some black parts on the surfaces. According to the chemical composition analysis using EDX, Mo was detected in the black parts, originating from the oxidization of the Mo crucible during crystal growth. However, Mo deposition was observed only on the surfaces of the as-grown crystals, and there was no Mo inside the crystals.

In the case of spring-shaped sapphire single crystals grown using the Mo crucible with the conical die under the growth condition of helical radius = 1.5 mm and helical pitch = 10.0 mm, the shape of the cross-sectional plane was almost circle [Fig.5(a)]. However, the cross-sectional planes under the growth conditions of helical radius > 1.5 mm became elliptical in shape, extending in the *Z*-axis direction owing to the spread of the meniscus during crystal growth. The elliptical shape of the single crystal under the growth conditions of helical radius = 3.5 mm and helical pitch = 10.0 mm was almost consistent with that of the helical radius = 3.0 mm and helical pitch = 5.0, 10.0 mm, suggesting that the menisci during the crystal growth of the three spring-shaped single crystals were almost the same shape.

Figure 5(b) shows the cross-sectional planes perpendicular to the growth direction for spring-shaped sapphire single crystals grown using a Mo crucible with an inverted conical die. The cross-sectional planes were elliptical and extended along the horizontal direction (*XY*-axes), contrary to the crucible with the conical die. The shape of the cross-sectional plane changed with the variation in the helical pitch and became thinner with decreasing helical pitch because of the tilting of the growth direction.

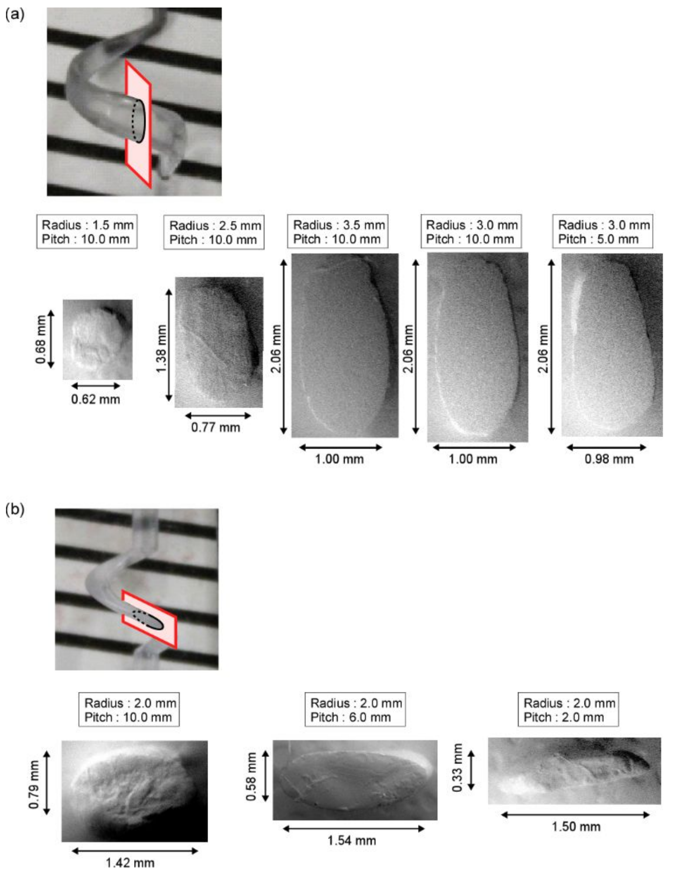

Fig. 5 SEM images on cross-sectional planes of spring-shaped sapphire single crystals grown using Mo crucibles with (a) the sharp conical die and (b) the inversed conical die.

Figure 6 shows schematic diagrams of the crystal growth using Mo crucibles with a sharp conical die and an inverse conical die. In the case of crystal growth using the Mo crucible with the conical die [Fig.6(a)], the area of the solid-liquid interface decreased and became stable when the die was sharpened. In particular, with the sharp conical die, the area of the solid-liquid interface increased by tilting the growth direction until the meniscus reached the edge of the die. Consequently, the cross-sectional planes of spring-shaped sapphire single crystals grown using crucibles with conical dies were elliptical and extended along the vertical (*Z*-axis) direction.

However, in the case of the Mo crucible with the inverse conical die, the meniscus spread only on the bottom of the die [Fig.6(b)], and the shape of the cross-sectional plane changed similarly with the variation in the helical pitch. According to the schematic diagram, the horizontal thickness of the meniscus did not change with the tilting of the growth direction. However, tilting in the growth direction reduces the vertical thickness of the meniscus, resulting in a horizontally extended elliptical cross-sectional plane. Therefore, the meniscus shifted from the capillary position at a helical pitch of < 2 mm, and the melt supply from the inside of the crucible was interrupted, making it impossible to grow a spring-shaped single crystal.

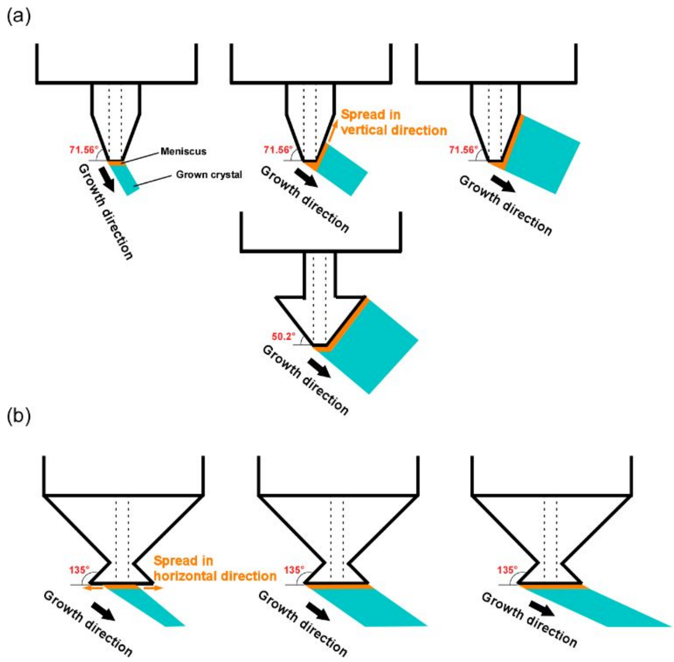

Fig. 6 Schematic diagrams of crystal growth using the Mo crucibles with (a) the sharp and blunt conical dies and (b) the inversed conical die.

4.4 Crystallinity

Pole figure and XRC measurements were performed to evaluate the crystallinity of the spring-shaped sapphire single crystals grown using Mo crucibles with conical and inverse conical dies. Figure 7 shows the pole figure and XRC from the reflection of the (110) plane on the cross-sectional plane of spring-shaped sapphire single crystals grown using a crucible with a sharp conical die and an inverted conical die. Pole figures were obtained at four locations on a spring-shaped sapphire single crystal grown using a Mo crucible with an inverse conical die, as shown in Fig.7(a). A sharp diffraction peak can be observed in each pole figure, and all the diffraction peaks appear in the same direction. The results revealed that the obtained crystal was spring-shaped single crystal with a single crystallographic orientation. The crystallographic orientation of the spring-shaped sapphire single crystals can be determined from the seed crystal. A sharp diffraction peak was observed for a spring-shaped sapphire single crystal grown in a Mo crucible with a conical die.

Figure 7(b) is ω scans of the XRCs on the diffraction spots from the reflection of (110) plane at two different points for the spring-shaped sapphire single crystals grown using the Mo crucibles with the conical die. In both the XRCs, a symmetrical single peak was observed, and the results revealed no mosaic structure or slightly oriented gains. The full width at half maximum (FWHM) of the peak at No.1 point for the spring-shaped sapphire single crystals grown using Mo crucibles with a conical die was 83 arcsec (0.023°), which was slightly larger than that of the sapphire single crystal grown by the conventional μ-PD method[14]. However, the XRC at No.3 point showed a symmetrical broader single peak with an FWHM of 152 arcsec (0.042°), indicating that the spring-shaped sapphire single crystal had different crystallinity at each location. The results suggested that spring-shaped single crystals grown from the meniscus spread in the vertical direction with a larger temperature gradient showed lower crystallinity than those grown from the meniscus spread in the horizontal direction with a more uniform temperature distribution in the conventional μ-PD method.

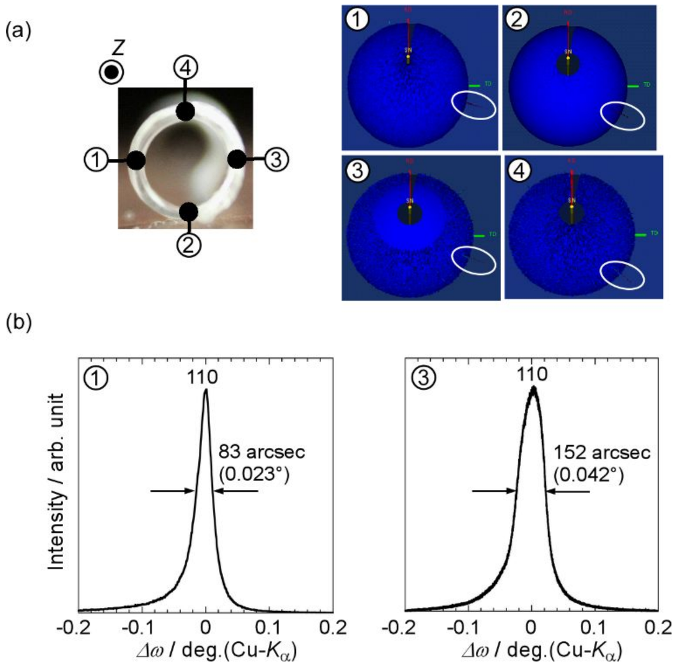

Fig. 7 (a) Pole figures obtained at four locations on the spring-shaped sapphire single crystal grown using the Mo crucible with the inversed conical die. (b) X-ray rocking curves of spring-shaped sapphire single crystals.

4.5 Mechanical Property

The mechanical properties of spring-shaped sapphire single crystals grown using Mo crucibles with conical and inverse conical dies were evaluated. Figure 8 shows spring-shaped single crystals before and after compression. For a spring-shaped sapphire single crystal grown using a Mo crucible with a conical die, the shrinkage was approximately 0.3 mm for the helical radius of 3 mm and helical pitch of 6 mm, and the shrinkage rate was approximately 5% just before the destruction. However, the spring-shaped sapphire single crystal grown using the Mo crucible with the inversed conical die showed a shrinkage of approximately 0.75 mm for the helical radius of 2 mm and helical pitch of 2 mm and the shrinkage rate was approximately 35% just before the destruction. The difference in shrinkage rates between crystals grown using a Mo crucible with conical and inverse conical dies can be attributed to the difference in the cross-sectional shape; thus, greater shrinkage can be achieved by forming spring-shaped single crystals with a thinner cross-sectional shape in the *Z*-axis direction. In addition, in terms of the compression test force, spring-shaped single crystals with a thinner cross-section in the *Z*-axis direction can achieve a greater shrinkage rate with less compression force.

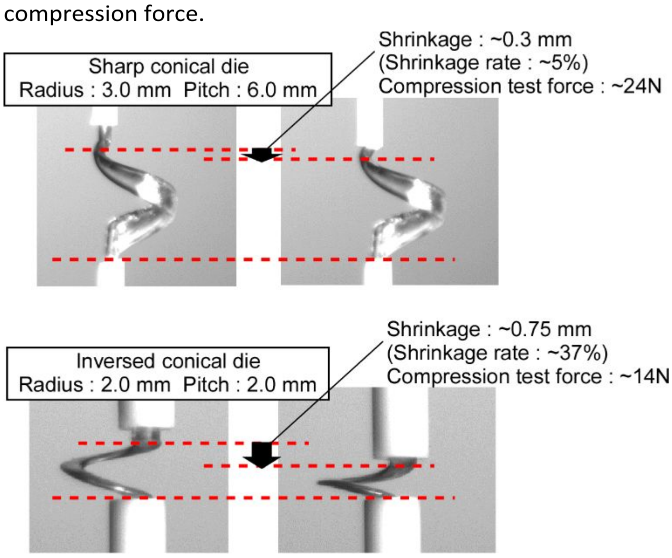

Fig. 8 Spring-shaped single crystals grown using Mo crucibles with the sharp and inversed conical dies before and after compression.

5. Conclusions

A 3D-μ-PD method was developed in this study for crystal growth of 3D shape-controlled single crystals. In particular, spring-shaped sapphire single crystals were grown by the 3D-μ-PD method using the Mo crucibles with three types dies. In the crystal growth using the crucible with the conical die, spring-shaped sapphire single crystals with smaller helical pitch could be grown by the crucible with the sharp conical die compared to the crucible with the blunt conical die. In addition, a crucible with an inverted conical die enabled the growth of a spring-shaped sapphire single crystal with a small helical pitch. The difference in meniscus spreading between the crucible with the conical and inverse conical dies affects the shape of the cross-sectional planes of the grown spring-shaped single crystals, resulting in differences in crystallinity and mechanical properties. Spring-shaped sapphire single crystals with a thin cross-sectional plane in the *Z*-direction achieved a higher shrinkage rate, and spring-shaped functional single crystals are expected to acquire springiness.

If a spring-shaped piezoelectric single crystal can be grown as a potential application for spring-shaped crystals, it is expected that springs and sensing devices that can generate vibration power will be realized. In addition, spring-shaped scintillator single crystal can be applied to springs with radiation detection functions and radiation detectors with three-dimensional position sensitivity.

Author contributions

Yuui Yokota: conceptualization, supervision, writing– original draft, review and editing, Investigation and methodology; Yuji Ohashi and Akira Yoshikawa: formal analysis and discussion. All authors have read and agreed to the published version of the manuscript.

Conflicts of interest

There are no conflicts of interest to declare.

Data availability

The data supporting this article have been included as part of the Supplementary Information.

Acknowledgements

This study was partially supported by the Japan Society for the Promotion of Science (JSPS) KAKENHI, Grant-in-Aid for Scientific Research [19H02795], Japan Science and Technology Agency (JST), Adaptable & Seamless Technology Transfer Program through Target-driven R&D (A-STEP) [AS272S003a], and the Grant Program of the Sumitomo Foundation.

Notes and references

1 J. Czochralski and Z. Phys. Chem. 1917, **92**, 219.
2 Y. Yokota, Y. Ohashi, T. Kudo, V. V. Kochurikhin, A. Medvedev, S. Kurosawa, K. Kamada and A. Yoshikawa, *J. Cryst. Growth* 2017, **468**, 321–325.
3 P. W. Bridgman, *Proc. Am. Acad. Arts Sci.* 1925, **60**, 305–383.
4 D. C. Stockbarger, *Rev. Sci. Instrum.* 1936, **7**, 133.
5 S. Kimura and K. Kitamura, *J. Am. Ceram.* 1992, **75**, 1440–1446.
6 A. M. Balbashov and S. K. Egorov, *J. Cryst. Growth* 1981, **52**, 498–504.
7 H. E. LaBelle Jr. and A. I. Mlavsky, *Mater. Res. Bull.* 1971, **6**, 571–579.
8 H. Machida, K. Hoshikawa and T. Fukuda, *J. Cryst. Growth* 1993, **128**, 829–833.
9 V. N. Kurlov and B.M. Epelbaum, *J. Cryst. Growth* 1998, **187**, 107-110.
10 D. Garcia, M. Ouellette, B. Mackintosh and J. P. Kalejs, *J. Cryst. Growth* 2001, **225**, 566–571.
11 V. N. Kurlov, N. V. Klassen, A. M. Dodonov, S. Z. Shmurak, G. K. Strukova, I. M. Shmyt'ko, S. E. Derenzo and M. J. Weber, *Nucl. Instrum. Methods Phys. Res. A* 2005, **537**, 197–199.
12 V. I. Chani and T. Fukuda, *Shaped Crystals: Growth by Micro-Pulling-Down Technique*, Springer, Berlin, Heidelberg, 2007.
13 Y. Yokota, M. Yoshino and T. Horiai, *Inorganic Scintillator and Crystal Growth Methods*, Wiley-VCH GmbH, Weinheim, Berlin, 2024.
14 Y. Yokota, V. Chani, M. Sato, K. Tota, K. Onodera, T. Yanagida and A. Yoshikawa, *J. Cryst. Growth* 2011, **318**, 983–986.
15 Y. Yokota, S. Kurosawa, Y. Ohasi, K. Kamada and A. Yoshikawa, *J. Cryst. Growth* 2016, **452**, 69–72.
16 Y. Yokota, M. Sato, V. Chani, Y. Futami, K. Tota, S. Kurosawa, K. Onodera and A. Yoshikawa, *Sens. Actuators. A Phys.* 2013, **200**, 56–59.
17 Y. Yokota, A. Yoshikawa, Y. Futami, M. Sato, K. Tota, K. Onodera and T. Yanagida, *IEEE Trans. Ultrason. Ferroelectr. Freq. Control* 2012, **59**, 1868–1871.
18 Y. Yokota, M. Sato, Y. Futami, K. Tota, T. Yanagida, K. Onodera and, A. Yoshikawa, *J. Cryst. Growth* 2012, **352**, 147–150.
19 Y. Yokota, M. Sato, K. Tota, Y. Futami, T. Yanagida, K. Onodera and A. Yoshikawa, *Jpn. J. Appl. Phys.* 2011, **50**, 09ND03.
20 Y. Yokota, T. Nihei, K. Tanaka, K. Sakairi, V. Chani, Y. Ohashi, S. Kurosawa, K. Kamada and A. Yoshikawa, *Adv. Eng. Mater.* 2017, **20**, 1700506.
21 Y. Yokota, T. Nihei, S. Abe and A. Yoshikawa, *Adv. Eng. Mater.* 2021, **23**, 2100144.
22 C. Dujardin, C. Mancini, D. Amans, G. Ledoux, D. Abler, E. Auffray, P. Lecoq, D. Perrodin, A. Petrosyan and K. L. Ovanesyan, *J. Appl. Phys.* 2010, **108**, 013510.
23 P. Rudolph and T. Fukuda, *Cryst. Res. Technol.* 1999, **34**, 3–40.
24 Y. Yokota, S. Kurosawa, Y. Shoji, Y. Ohashi, K. Kamada and A. Yoshikawa, *Opt. Mater.* 2017, **65**, 46–51.
25 Y. Yokota, Y. Fujimoto, T. Yanagida, H. Takahashi, M. Yonetani, K. Hayashi, I. Park, N. Kawaguchi, K. Fukuda, A. Yamaji, Y. Fukazawa, M. Nikl and A. Yoshikawa, *Cryst. Growth Des.* 2011, **11**, 4775–4779.

Data availability statements

The data supporting this article have been included as part of the Supplementary Information.

Yuui Yokota

Associate Professor
Institute for Materials Research,
Tohoku University

2-1-1, Katahira, Aoba-ku, Sendai, 980-8577, JAPAN
TEL +81-22-215-2214
FAX +81-22-215-2215
E-mail yui.yokota.a5@tohoku.ac.jp